Mechanisms of elevation-dependent warming over the Tibetan plateau in quadrupled CO_2 experiments

Libin Yan, Zhengyu Liu, Guangshan Chen, J. E. Kutzbach & Xiaodong Liu

Climatic Change
An Interdisciplinary, International Journal Devoted to the Description, Causes and Implications of Climatic Change

ISSN 0165-0009

Climatic Change
DOI 10.1007/s10584-016-1599-z

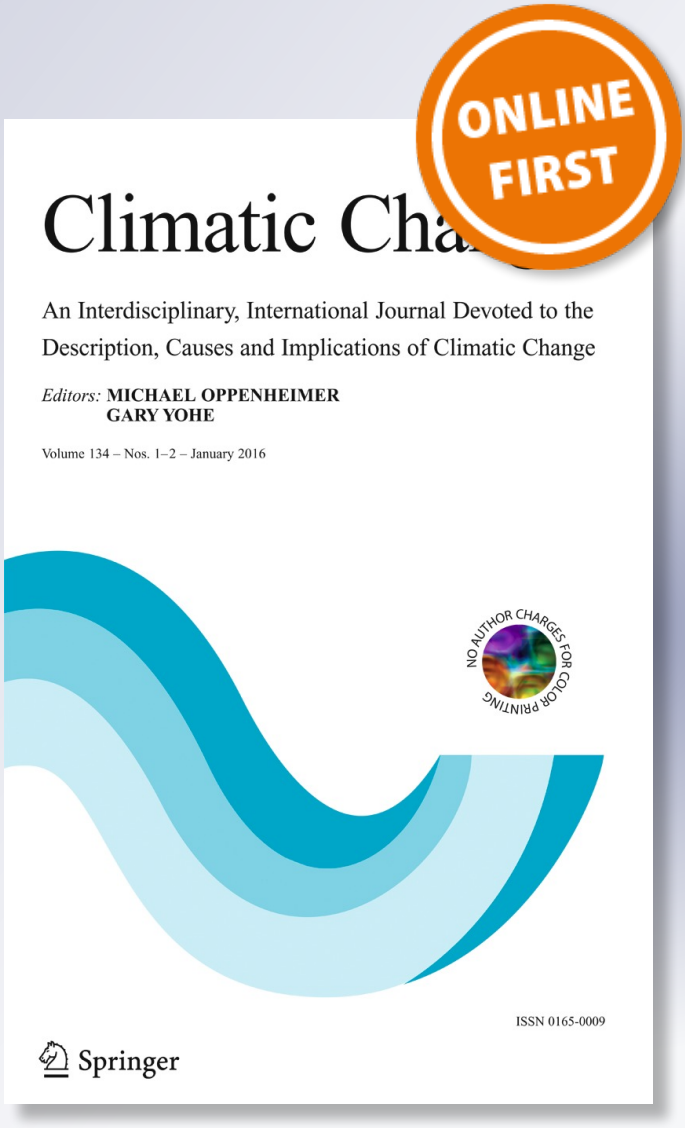

Springer

Climatic Change
DOI 10.1007/s10584-016-1599-z

Mechanisms of elevation-dependent warming over the Tibetan plateau in quadrupled CO_2 experiments

Libin Yan[1] · **Zhengyu Liu**[2] · **Guangshan Chen**[2] · **J. E. Kutzbach**[2] · **Xiaodong Liu**[1]

Received: 9 September 2015 / Accepted: 3 January 2016

Abstract Observations have shown that the Tibetan Plateau (TP) has experienced elevation-dependent warming (EDW) during recent decades, that is, greater warming at higher elevations than at lower elevations. However, the factors and their mechanisms driving these changes remain unclear, due to scarce radiation-related observations. In the present study, four CCSM3 experiments using the 1990 control and quadrupled (4×) CO_2 levels, with fine and coarse resolutions, were examined to shed light on the mechanisms driving EDW. The differences in annual and seasonal surface temperatures (TS) between the 4× CO_2 and 1990 control runs, using T85 resolution, feature clear changes with elevation. In addition, EDW 500 m above the ground surface is much weaker and almost disappears at the surface elevations higher than 2000 m. This implies that the greater warming mainly occurs at the near surface with higher elevations and should be attributed to changes in the surface energy budget. In the 4× CO_2, there are greater increases (compared to the 1990 control run) in the net solar, net longwave and sensible heat fluxes at the surface at higher elevations, but lower levels of the parameters are simulated at lower elevations. These differences lead to increases in the heat storage at the surface and finally result in greater warming at higher elevations. Compared with the net longwave flux, the relative net shortwave flux at the surface increases more evidently at higher elevations, implying that the increase in net shortwave flux at the surface plays a dominant role in producing greater warming at higher elevations. The elevation range between 2000 and 3000 m appears to be a turning point; below 2000 m, the total cloud increases and subsequently constrains the surface net solar radiation. Above 3000 m, the total cloud decreases but shows little elevation dependency, favoring the increases in the surface net solar radiation, and decreases in the snow depth, with more differences with increasing elevation, lead to the reduced surface albedo. This further facilitates

✉ Libin Yan
yanlibin@ieecas.cn

[1] SKLLQG, Institute of Earth Environment, Chinese Academy of Sciences, Xi'an 710061, China

[2] Center for Climatic Research, University of Wisconsin-Madison, 1225 West Dayton St,, Madison, WI 53706, USA

Published online: 11 January 2016

the absorption of solar radiation at higher elevations. Therefore, the combined effects of changes in the snow depth and cloud cover in response to 4× CO_2 levels result in greater heat storage at the surface at higher elevations than at lower elevations, leading to EDW over and around the TP.

1 Introduction

As the highest and largest highland in the world, the Tibetan Plateau (TP) profoundly impacts regional and global climates through thermal and mechanical forcing (An et al. 2001; Yanai and Wu 2006). At the same time, the TP is sensitive and vulnerable to climatic change (Messerli and Ives 1997); as a result, trends observed in its climate can be seen as an early warning signal of global change. During recent decades, the TP has experienced more rapid warming than its vicinity (Kang et al. 2010; Liu and Chen 2000; Rangwala and Miller 2012), especially since the start of the 21st century (Yan and Liu 2014) and in future (Ji and Kang 2012). Moreover, climatic warming over the TP is dependent on elevation (Liu and Chen 2000; Liu et al. 2009; Pepin et al. 2015; Yan and Liu 2014), that is, warming has occurred at a greater rate at higher elevations. This elevation-dependent warming (EDW) may continue into the future (Liu et al. 2009; Rangwala et al. 2013).

There is growing evidence demonstrating that global warming can mainly be attributed to the increases in greenhouse gases emissions (Solomon 2007). More significant warming over the TP is captured in climate models when they are forced by observed CO_2 concentrations, rather than by the fixed external conditions before the industrial revolution (Duan et al. 2006). Scenarios representing an annual 1 % increase in CO_2 and the IPCC mid-range CO_2 emissions (A1B) have both been shown to cause greater warming over the higher TP region (Liu et al. 2009). Hence, conclusions that the increasing greenhouse gases have probably caused the warming observed over and around the TP have been made. The greater warming observed at higher elevations has been attributed to a variety of mechanisms (Pepin et al. 2015; Rangwala and Miller 2012), including snow-albedo feedback (Liu et al. 2009), cloud cover (Duan and Wu 2006; Liu et al. 2009), water vapor modulation of longwave heating (Rangwala et al. 2009), surface water vapor (Rangwala et al. 2015) and aerosols (Lau et al. 2010). However, these mechanisms need further investigation (Kang et al. 2010; Yang et al. 2014), which has motivated us to investigate how increased CO_2 levels affect the surface energy budget and result in EDW over the TP.

There are few observational stations over the higher TP and, as a result, observations of surface radiative processes are scarce. However, climate models provide an efficient way to investigate the mechanisms by which EDW occurs in response to increased CO_2; this has become especially true as the parameterization schemes have improved and finer resolutions have been enabled in climate models. For example, Ji and Kang (2013) found that the high resolution climate modelling can capture the spatial-temporal features of temperature and precipitation better, and conducted projection of future climate change on the TP. The analyses of annual 1 % increases in CO_2 levels, using the Community Climate System Model 3 (CCSM3), showed that more significant warming at higher elevations on the TP resulted from a greater increase in absorbed solar radiation, but lesser increase in downward longwave radiation, near the ground surface, from low-elevation to high-elevation regions (Liu et al. 2009). However, changes in the surface energy budget processes have not been comprehensively studied

in recent literature. For example, the radiation factors which contribute more to the greater warming at higher elevations on the TP in response to increased CO_2 concentration level and the physical processes have not been determined. Therefore, this study aims to investigate EDW in response to quadrupled (4×) CO_2 levels using the CCSM3, with a fine and coarse resolution, and attempts to unveil the effects that changes in the surface energy budget processes have in terms of driving amplified warming over the higher elevations of the TP.

Details of the modeling experiments and the analytical methods are provided in Section 2. Section 3 describes the simulated EDW over and around the TP and unveils the mechanisms driving it, through diagnosis of the surface energy budget. A discussion is provided in Section 4.

2 Data and methods

The CCSM3 is a widely used climate model and serves as a powerful tool for advancing our understanding of climate change. A series of CCSM3 experiments (http://www.cesm.ucar.edu/experiments/ccsm3.0/) were carried out and are available to the public. The experiments included five prescribed scenarios (1990 control, 1 % increasing CO_2, 2× CO_2, 4× CO_2 and 1870 control) and three different model resolutions (T85, T42 and T31). The output data of these experiments were distributed via the Earth System Grid (ESG). Tian and Jiang (2013) reported that the CCSM model performs well in capturing the characterization of surface air temperature over East Asia and China. In this study, four of the experiments were used, including the 1990 control and 4× CO_2 runs under the T85 and T31 resolutions respectively. In the 1990 control runs, the CO_2 concentrations were fixed at 355 ppmv, and in the 4× CO_2 runs, the CO_2 concentrations were quadrupled to 1420 ppmv. The truncated T85 and T31 spectral resolutions had grid spacings of 1.4° and 3.75°, respectively. The four experiments were run for various time spans (all multi-century simulations), but the averages of the last fifty years were used to represent the mean patterns in each experiment. The differences between the mean patterns of the 4× CO_2 and 1990 control runs were used to indicate the effects of CO_2 on the climate, and facilitate us to investigate the mechanisms driving EDW over the mountainous regions.

The focus of this study was the TP and its vicinity (70°–105°E, 26°–42°N; Fig. 1a and 1b). The topography in the T85 and T31 resolution runs both depicted the elevation gradient from the lower surroundings to the higher center of the TP, but the T85 resolution captured the detailed topography of the TP more accurately than the T31 resolution. To detect the EDW over the TP, the study area was divided into 11 zones based on elevation (0.5 km height intervals). For the T85 resolution runs, each zone contained 20 or more model grid cells (Fig. 1c), while for the T31 resolution runs only 9 of the zones had 3 or more model grid cells, due to the coarser resolution (Fig. 1d); the grid-mean elevation of each zone in the T85 and T31 resolution runs represented the gradual increase in elevation (Fig. 1c and d). The differences in surface temperature (TS) between the mean patterns in the 4× CO_2 and 1990 control runs, from the lower to the higher elevation zones, were used to shed light on whether EDW exists at the ground surface under the impact of 4× CO_2. An analysis to identify whether EDW occurs 500 m above the ground surface was similarly conducted.

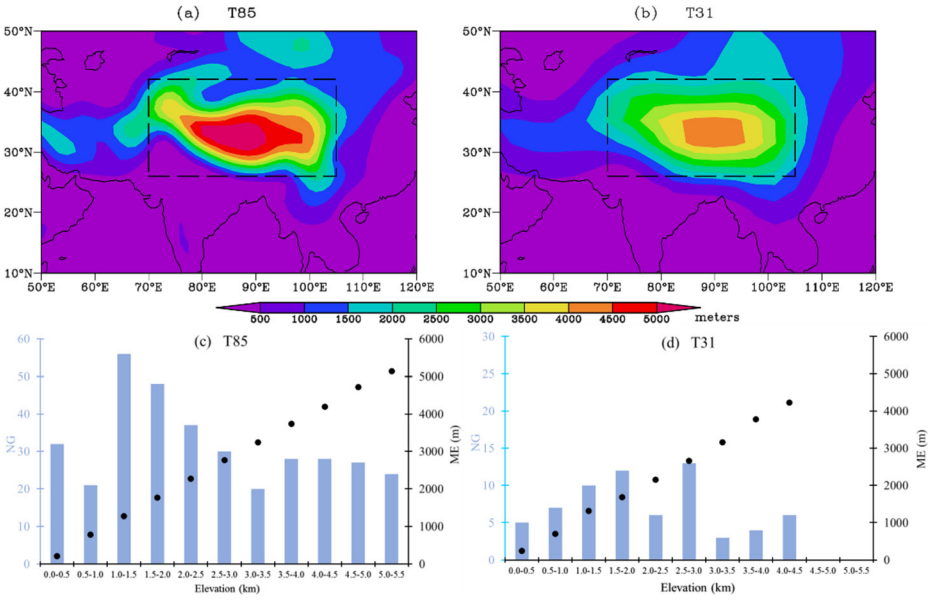

Fig. 1 Topography (m) in the T85 (a) and T31 (b) resolution experiments. The dashed boxes (70°–105°E, 26°–42°N) denote the TP domain. (c) and (d) show the number of model grid cells (NG, blue bars) and corresponding grid-mean elevations (ME, black dots) for each elevation zones over the TP domain in the T85 (c) and T31 (d) resolution experiments

The changes in the surface energy budget in response to 4× CO_2 were diagnosed following the methods of Lu and Cai (2009). The surface energy budget can be written as:

$$\begin{aligned} Q &= S^{\downarrow} - S^{\uparrow} + F^{\downarrow} - F^{\uparrow} - H - LE \\ &= S_{net} + F_{net} - H - LE \end{aligned} \tag{1}$$

where Q is the heat storage term at the surface. $S^{\downarrow}$ and $S^{\uparrow}$ are surface downward and upward shortwave radiation. $F^{\downarrow}$ and $F^{\uparrow}$ are surface downward and upward longwave radiations. S_{net}, F_{net}, H and LE represent the net shortwave radiative flux at the surface, the net longwave flux at the surface, the surface sensible heat flux and the surface latent heat flux, respectively. S_{net}, F_{net}, H and LE are directly obtained from the CCSM3 model outputs. Q is calculated based Eq. (1). The differences in these radiative variables between the 4× CO_2 and 1990 runs were examined to reveal their role in driving the greater warming simulated at higher elevations. Finally, in order to find the mechanisms that were forcing the changes in the surface energy budget, differences in radiation-related variables of CCSM3 were also examined.

3 Results

3.1 Characterization of elevation-dependent warming

The annual (ANN) and seasonal (March–April–May, MAM; June–July–August, JJA; September–October–November, SON; and December–January–February, DJF) differences in TS between the 4× CO_2 and 1990 control runs, simulated using the T85 resolution, are

elevation-dependent (Fig. 2). The annual TS differences, simulated using the T85 resolution, increase from about 4 °C at lower elevations to about 7 °C at higher elevations. Within each season, the TS differences all increase as the elevation increases; this implies that the differences in the TS in response to 4× CO_2 are elevation-dependent, at both the annual and seasonal timescales. At the seasonal scale, the EDW is most evident in spring, followed by summer and autumn, and is least evident in winter.

Compared with the T85 resolution, the EDW simulated using the T31 resolution is not consistent at either the annual or seasonal timescale. For example, the TS difference between

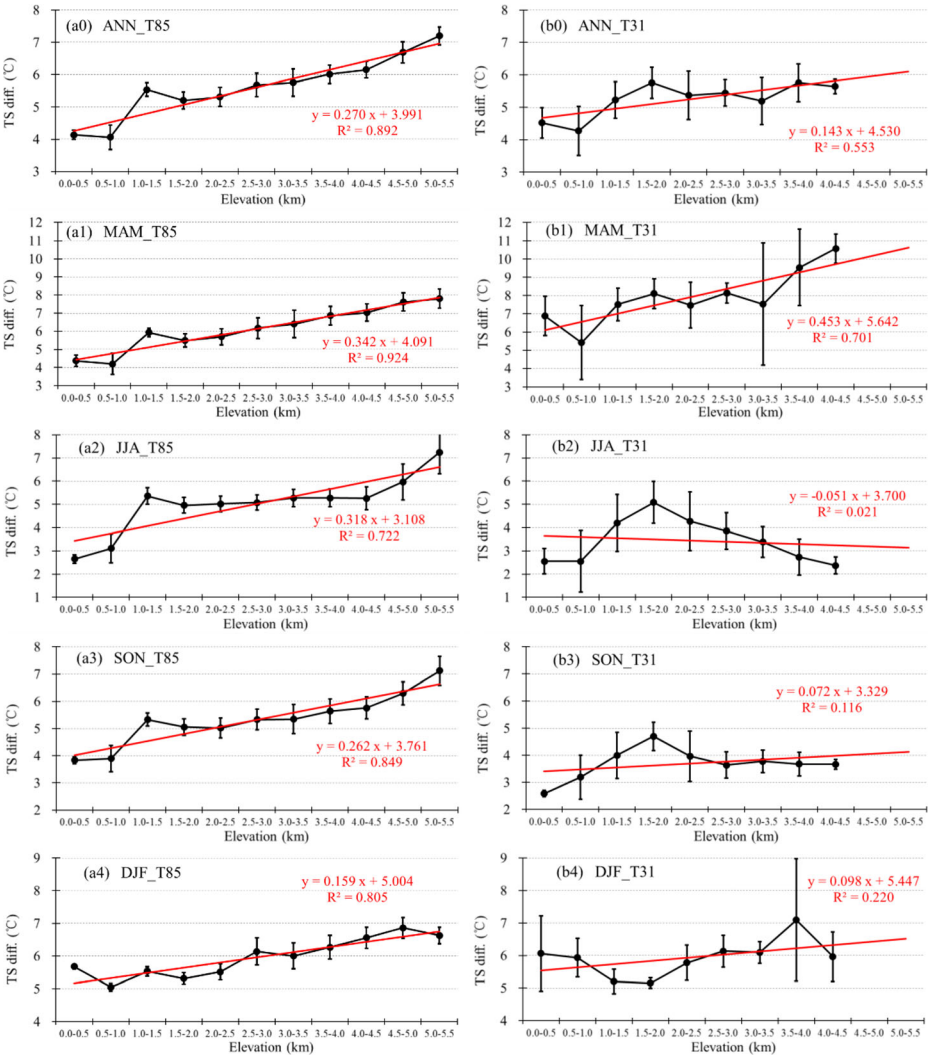

Fig. 2 The differences in surface temperatures (TS diff.) between the 4× CO_2 and 1990 control runs simulated using the T85 (a0–4) and T31 (b0–4) resolutions, at the annual (ANN; a0, b0) and seasonal (March–April–May, MAM, a1, b1; June–July–August, JJA, a2, b2; September–October–November, SON, a3, b3; and December–January–February, DJF, a4, b4) scales. Red lines and numbers denote the linear relationships between the TS difference and elevation. Black error bars represent the standard deviation of the TS difference at each elevation

the 4× CO_2 and 1990 control runs, simulated by the T31 resolution in summer, autumn and winter does not increase with elevation. However, there is a slight and evident increase in the TS difference at the annual scale, and in spring, respectively. Overall, the results imply that the low resolution climate model is not able to capture EDW over and around the TP.

The temperature differences 500 m above the ground surface (between the 4× CO_2 and 1990 control runs) simulated using both the T85 (Fig. 3a) and T31 (Fig. 3b) resolutions, show that although the temperature differences 500 m above the ground surface when the ground level elevation is higher than 1 km, appear greater than when it is lower than 1 km (in both the T85 and T31 resolution runs), the differences feature weaker EDW, especially when the ground surface is above 2 km elevation. The results imply that EDW is a near surface phenomenon, and does not occur 500 m above the ground surface; therefore, the greater warming that is apparent (in response to 4× CO_2) at the near surface at higher elevations, in comparison to lower elevations, should be attributed to changes in the surface energy budget.

3.2 Elevation-dependent changes in the surface energy budget

To investigate the mechanisms driving EDW over the TP, the changes in surface energy budget in response to 4× CO_2 at different elevations were examined (Fig. 4). Using the T85 resolution, compared with the 1990 control run, the net solar flux (Fig. 4a1) and net longwave flux (Fig. 4a2) at the surface in the 4× CO_2 run are clearly larger at higher elevations, but smaller at lower elevations, and thus are elevation-dependent. The elevation range between 2000 and 3000 m appears to be the turning point. Above 3000 m, the net solar flux and longwave flux both are both larger in the 4× CO_2 run than in the 1990 control run (and the difference increases with increasing elevation). In contrast, both parameters are lower in the 4× CO_2 run when the elevation is below 2000 m. The same elevation-dependent pattern (at similar elevations) is seen in the surface sensible heat flux (Fig.4a3), resulting from the differences in the elevation-dependent net solar and net longwave fluxes. In contrast, the surface latent heat flux (Fig.4a4) is not elevation-dependent.

The heat storage at the surface (Fig. 4a5) is clearly elevation-dependent, with greater differences in the ground surface heat storage at higher elevations, compared to at lower elevations, between the 4× CO_2 and 1990 control run results. This response leads to the greater warming at higher elevations (Fig. 2a0). In addition, compared with the net longwave flux at the surface (Fig. 4a2), the increases in the net shortwave flux at the surface (Fig. 4a1) are more evident at higher elevations. This implies that the increase in net shortwave flux at the surface plays a dominant role in producing the greater warming simulated at higher elevations.

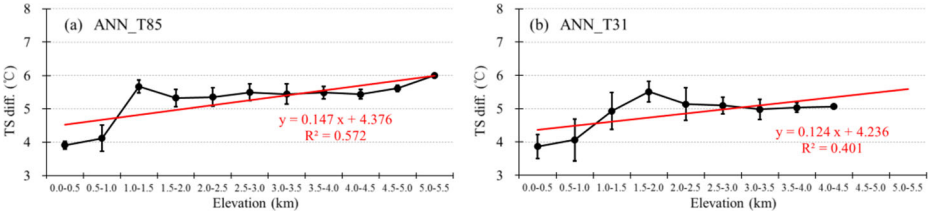

Fig. 3 The differences in temperature above the ground surface (~ 500 m) between the 4× CO_2 and 1990 control runs, simulated using the T85 (a) and T31 (b) resolutions, at the annual (ANN) scale

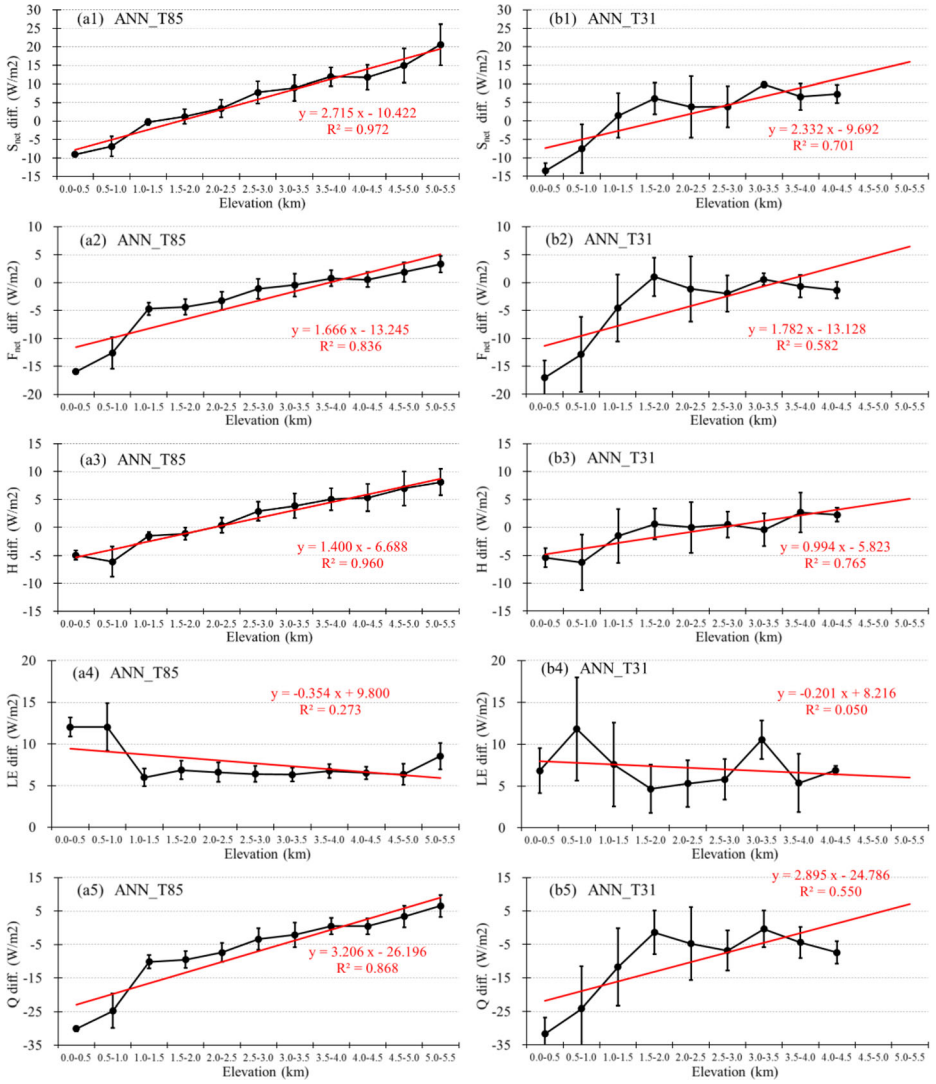

Fig. 4 The differences in annual (ANN) net solar flux at the surface (S_{net}; a1, b1), net longwave flux at the surface (F_{net}; a2, b2), the surface sensible heat flux (H; a3, b3), the surface latent heat flux (LE; a4, b4) and the heat storage term at the surface (Q; a5, b5) between the 4× CO_2 and 1990 control runs, using the T85 (a1–5) and T31 (b1–5) resolutions, at each elevation

In the T31 resolution runs (Fig. 4b1–5), the model did not capture the elevation dependencies observed in the surface radiation fluxes using the T85 resolution. The net solar (Fig. 4b1) and longwave (Fig. 4b2) fluxes simulated in these runs do not appear to be very elevation-dependent from 2000 to 4500 m. Although, the differences in the fluxes, between the two CO_2 scenarios, do increase from 0 to 2000 m. Overall, the 4× CO_2 run using the T31 resolution clearly fails to capture the same changes in surface energy budget above 2000 m, compared with the T85 resolution.

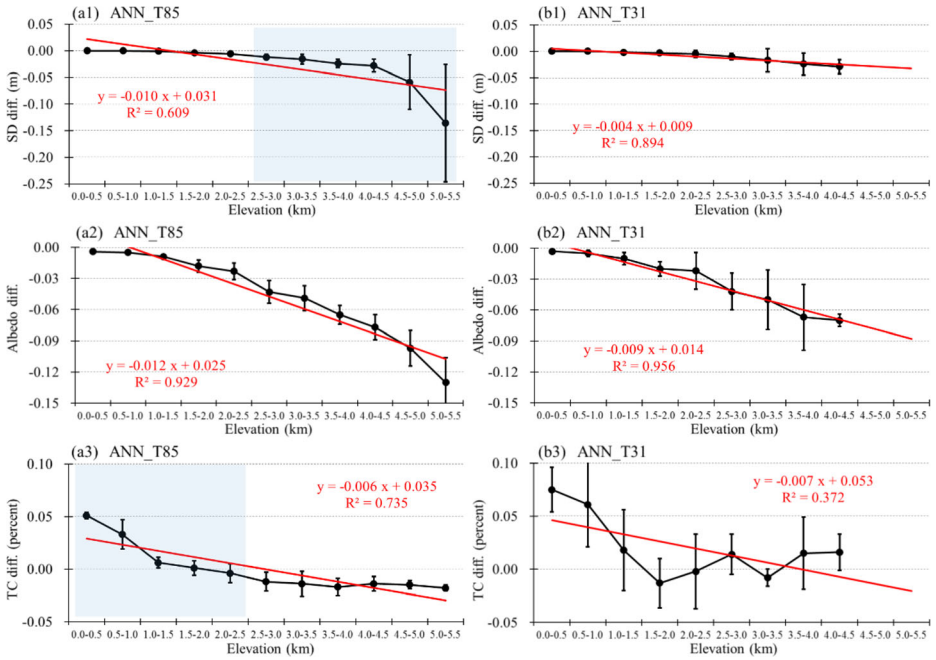

Fig. 5 The differences in the annual (ANN) snow depth (SD; a1, b1), surface albedo (a2, b2) and total cloud (TC; a3, b3) between the 4× CO_2 and 1990 control runs, simulated using the T85 (a) and T31 (b) resolutions, at each elevation

3.3 The mechanisms forcing the elevation-dependent changes in the ground surface energy budget

Differences in the snow depth and total cloud are the main driving factors that influence the surface energy budget; the differences in both factors between the 4× CO_2 run relative to the control run, change with elevation (Fig. 5). Using the T85 resolution, the differences in snow depth (SD diff., Fig. 5a1) and total cloud (TC diff., Fig.5a3) between the 4× CO_2 run and 1990 control run both exhibit negative correlations with elevation. In the 4× CO_2 run the simulated snow depth is lower than in the 1990 control run at elevations higher than 3000 m (the differences increase with elevation, but are not noteable at lower elevations). The greater decrease in snow depth in the 4× CO_2 run (compared to the 1990 control run) is caused by the greater increase in TS differences at the higher elevation; in turn, this results in a reduced difference in the surface albedo (Fig. 5a2, the ratio of $S^{\uparrow}$ to $S^{\downarrow}$ at surface) and further enhances the absorption of solar radiation (Fig. 4a1) at higher elevations. This demonstrates the important role of snow-albedo feedback mechanisms in amplifying the warming at higher elevations (Giorgi et al. 1997; Liu et al. 2009).

Although the total cloud levels increase overall, the differences between the 4× CO_2 run and 1990 control run decrease with elevation, at elevations lower than 2000 m. Above 3000 m elevation, although the total cloud levels decrease, there is little effect of elevation between the two scenarios. The increase in total cloud levels at lower elevations leads to decreased net solar (Fig. 4a1) and longwave (Fig. 4a2) radiation, while the decrease in total cloud at higher elevations favors increases in solar (Fig. 4a1) radiation. The combined effects of the changes in snow depth and cloud cover, in response to the 4× CO_2 levels, result in a larger increase in heat

storage at the surface (Fig. 4a5) at higher elevations than at lower elevations, which leads to EDW over and around the TP.

The poor performance of the changes in snow depth (Fig. 5b1) and total cloud (Fig. 5b3) in the runs using the T31 resolution, especially at higher elevations, may have led to the failure of these runs to capture the EDW and the related changes in surface energy budget, in response to 4× CO_2.

4 Discussion

The interesting phenomenon of EDW over the TP was detected in weather station observations, but its driving mechanisms remain unclear. In the present study, four CCSM3 experiments were examined to shed light on the mechanisms driving EDW, by simulating the response to 4× CO_2 concentrations. The results show that the differences in annual and seasonal TS between the 4× CO_2 and 1990 control runs, using the T85 resolution, feature clear trends with elevation. However, the EDW is not captured in the T31 resolution experiments, due to the poorer depiction of the topography over the TP. In addition, EDW at 500 m above the ground surface for each grid cell is not evident, implying that EDW mainly occurs at the ground surface, and the relative increases in near surface warming at higher elevations in response to the 4× CO_2 are attributed to changes in the surface energy budget.

In the 4× CO_2 run, greater increases (compared to the 1990 control run) in the net solar and net longwave radiation fluxes at the surface, at higher elevations are simulated, but lower levels of the parameters in the 4× CO_2 run are simulated at lower elevations. The elevation range between 2000 and 3000 m appears to be a turning point. Above 3000 m, the net solar, longwave and surface sensible heat fluxes are all higher in the 4× CO_2 run, but they are lower below 2000 m. In contrast, the surface latent heat flux is not elevation-dependent. Finally, the heat storage at the surface simulated in the 4× CO_2 scenario is higher, relative to that simulated in the 1990 control run and the difference increases with elevation, leading to greater warming. Compared with the net longwave flux at the surface, the net shortwave flux at the surface increases more evidently at higher elevations, implying that the increase in the net shortwave flux at the surface plays a dominant role in driving the greater warming at higher elevations. Meanwhile, the 4× CO_2 run performed using the T31 resolution fails to capture the changes in the radiation fluxes above 2000 m.

The changes in snow depth and total cloud appear to be the two main driving factors; for both parameters, the differences between the two scenarios correlate negatively with elevation. The relative decrease in snow depth in the 4× CO_2 scenario (compared to the 1990 control) mainly occurs at elevations higher than 3000 m, resulting in a reduction in the surface albedo and further increasing the absorption of solar radiation. Overall, the increases in total cloud at elevations lower than 2000 m, reduce the net solar and longwave radiation, and the overall decreases at elevations higher than 3000 m, which do appear to be elevation-dependent, increase the solar and longwave radiation. Finally, the combined effects of changes in snow depth and cloud cover, in response to the 4× CO_2 scenario, lead to greater heat storage at the surface at higher elevations, than at lower elevations, leading to EDW, in the simulations.

It should be noted that other factors, like surface water vapor (Rangwala et al. 2015), the surface versus free-air coupling (Pepin et al. 2011) and surface transpiration processes (Shen et al. 2015) also play important roles in producing EDW over and around the TP. However, it is apparent that the simulated EDW is initially caused by the 4× CO_2 concentrations in these

experiments. Conventionally, greenhouse gas forcing acts to reduce the outgoing longwave radiation and enhances net surface longwave radiation. However, in this study, the increase in shortwave radiation, resulting from the reduced snow depth and decreased cloud level, is a dominant factor that led to the greater warming at higher elevations, in response to the 4× CO_2 levels, which was also demonstrated by (Trenberth et al. 2009) and Donohoe et al. (2014) in other regions under climate warming. In addition, as the albedo decreases especially at higher elevations, the net solar radiation increases and results in more surface warming, and this in turn would enhance outgoing longwave radiation and lead to a less warming, while the net surface longwave radiation still increases at higher elevations in response to quadrupled CO_2 (Fig. 4). Moreover, the present study is a projection study of the climatic response to quadrupled CO_2 rather than an explanation of the recent EDW, because the net surface shortwave radiation on the TP increases in the quadrupled CO_2 experiments while over the past decades the surface solar radiation exhibited an decreasing trend (Tang et al. 2011; You et al. 2009). Lastly, it should also be noted that in paleo-climate modeling studies, coarser resolutions are generally selected in order to save computing time; this study indicates that using finer resolution models is important, because they depict the topography better, which affects changes in surface radiation-related processes, and the changing magnitude of TS in high moutainous regions.

Acknowledgments This work was jointly supported by the Strategic Priority Research Program of the Chinese Academy of Sciences (XDB03020601) and the National Natural Science Foundation of China (41420104008). Zhengyu Liu acknowledges support from Chinese MOST 2012CB955201 and NSFC (41130105).

References

An Z, Kutzbach JE, Prell WL, Porter SC (2001) Evolution of Asian monsoons and phased uplift of the himalaya–tibetan plateau since late miocene times. Nature 411:62–66

Donohoe A, Armour KC, Pendergrass AG, Battisti DS (2014) Shortwave and longwave radiative contributions to global warming under increasing CO2. Proc Natl Acad Sci 111:16700–16705

Duan A, Wu G (2006) Change of cloud amount and the climate warming on the tibetan plateau. Geophys Res Lett 33:L22704. doi:10.1029/2006gl027946

Duan A, Wu G, Zhang Q, Liu Y (2006) New proofs of the recent climate warming over the tibetan plateau as a result of the increasing greenhouse gases emissions. Chin Sci Bull 51:1396–1400

Giorgi F, Hurrell JW, Marinucci MR, Beniston M (1997) Elevation dependency of the surface climate change signal: a model study. J Clim 10:288–296

Ji Z, Kang S (2012) Projection of snow cover changes over China under RCP scenarios. Clim Dyn 41:589–600. doi:10.1007/s00382-012-1473-2

Ji Z, Kang S (2013) Double-nested dynamical downscaling experiments over the tibetan plateau and their projection of climate change under two RCP scenarios. J Atmos Sci 70:1278–1290. doi:10.1175/jas-d-12-0155.1

Kang S, Xu Y, You Q, Flügel W-A, Pepin N, Yao T (2010) Review of climate and cryospheric change in the tibetan plateau. Environ Res Lett 5:015101. doi:10.1088/1748-9326/5/1/015101

Lau WK, Kim M-K, Kim K-M, Lee W-S (2010) Enhanced surface warming and accelerated snow melt in the himalayas and tibetan plateau induced by absorbing aerosols. Environ Res Lett 5:025204

Liu X, Chen B (2000) Climatic warming in the tibetan plateau during recent decades. Int J Climatol 20:1729–1742

Liu X, Cheng Z, Yan L, Yin Z-Y (2009) Elevation dependency of recent and future minimum surface air temperature trends in the tibetan plateau and its surroundings. Glob Planet Chang 68:164–174. doi:10.1016/j.gloplacha.2009.03.017

Lu J, Cai M (2009) Seasonality of polar surface warming amplification in climate simulations. Geophys Res Lett 36(L16):704. doi:10.1029/2009gl040133

Messerli B, Ives JD (1997) Mountains of the world: a global priority. Parthenon publishing group, New York
Pepin N et al. (2015) Elevation-dependent warming in mountain regions of the world. Nature Climate Change 5
Pepin NC, Daly C, Lundquist J (2011) The influence of surface versus free-air decoupling on temperature trend patterns in the western United States. J Geophys Res 116:D10109. doi:10.1029/2010jd014769
Rangwala I, Miller JR (2012) Climate change in mountains: a review of elevation-dependent warming and its possible causes. Clim Chang 114:527–547. doi:10.1007/s10584-012-0419-3
Rangwala I, Miller JR, Russell GL, Xu M (2009) Using a global climate model to evaluate the influences of water vapor, snow cover and atmospheric aerosol on warming in the tibetan plateau during the twenty-first century. Clim Dyn 34:859–872. doi:10.1007/s00382-009-0564-1
Rangwala I, Sinsky E, Miller JR (2013) Amplified warming projections for high altitude regions of the northern hemisphere mid-latitudes from CMIP5 models. Environ Res Lett 8:024040. doi:10.1088/1748-9326/8/2/024040
Rangwala I, Sinsky E, Miller JR (2015) Variability in projected elevation dependent warming in boreal midlatitude winter in CMIP5 climate models and its potential drivers. Climate Dynamics. doi:10.1007/s00382-015-2692-0
Shen M et al. (2015) Evaporative cooling over the tibetan plateau induced by vegetation growth. Proc Natl Acad Sci U S A. doi:10.1073/pnas.1504418112
Solomon S (2007) Climate change 2007-the physical science basis: working group I contribution to the fourth assessment report of the IPCC vol 4. Cambridge University Press, Cambridge
Tang WJ, Yang K, Qin J, Cheng CCK, He J (2011) Solar radiation trend across China in recent decades: a revisit with quality-controlled data. Atmos Chem Phys 11:393–406. doi:10.5194/acp-11-393-2011
Tian Z, Jiang D (2013) Evaluation of the performance of low-to high-resolution CCSM4 over east Asia and China (in Chinese). Chin J Atmos Sci 37:171–186
Trenberth KE, Fasullo JT, Kiehl J (2009) Earth's global energy budget. Bull Am Meteorol Soc 90:311–323. doi:10.1175/2008bams2634.1
Yanai M, Wu G-X (2006) Effects of the tibetan plateau. In:The Asian Monsoon. Springer, New York, pp 513–549. doi:10.1007/3-540-37722-0_13
Yan L, Liu X (2014) Has climatic warming over the tibetan plateau paused or continued in recent years? J Earth, Ocean Atmos Sci 1:13–28
Yang K, Wu H, Qin J, Lin C, Tang W, Chen Y (2014) Recent climate changes over the tibetan plateau and their impacts on energy and water cycle: a review. Glob Planet Chang 112:79–91. doi:10.1016/j.gloplacha.2013.12.001
You Q, Kang S, Flügel W-A, Sanchez-Lorenzo A, Yan Y, Huang J, Martin-Vide J (2009) From brightening to dimming in sunshine duration over the eastern and central tibetan plateau (1961–2005). Theor Appl Climatol 101:445–457. doi:10.1007/s00704-009-0231-9